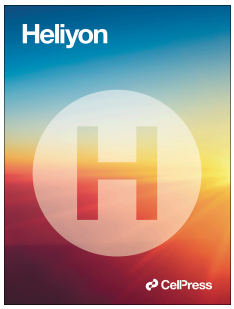

Long term adult visual plasticity after the developmental critical period in genetically determined *peripheral* visual loss

Otília C. d'Almeida, Joana M. Sampaio, Sonia Ferreira, Eduardo D. Silva, Miguel Castelo-Branco

PII: S2405-8440(25)00350-0

DOI: https://doi.org/10.1016/j.heliyon.2025.e41970

Reference: HLY 41970

To appear in: *HELIYON*

Received Date: 30 June 2024

Revised Date: 14 December 2024

Accepted Date: 13 January 2025

Please cite this article as: O.C. d'Almeida, J.M. Sampaio, S. Ferreira, E.D. Silva, M. Castelo-Branco, Long term adult visual plasticity after the developmental critical period in genetically determined *peripheral* visual loss, *HELIYON*, https://doi.org/10.1016/j.heliyon.2025.e41970.

Long term adult visual plasticity after the developmental critical period in genetically determined *peripheral* visual loss

Short title: Visual Plasticity in genetic visual loss

Otília C. d'Almeida[a,b], Joana M. Sampaio[a], Sonia Ferreira[a], Eduardo D. Silva[a], Miguel Castelo-Branco [a,b,c,*]

[a] Univ Coimbra, Coimbra Institute for Biomedical Imaging and Translational Research (CIBIT), Institute for Nuclear Sciences Applied to Health (ICNAS), Coimbra, Portugal

[b] Univ Coimbra, Faculty of Medicine, Coimbra, Portugal

[c] Univ Maastricht, Faculty of Psychology, Maastricht, The Netherlands

***Corresponding author:**

Professor Miguel Castelo-Branco, MD PhD
ICNAS – Institute of Nuclear Sciences Applied to Health
Pólo das Ciências da Saúde, Universidade de Coimbra
Azinhaga de Santa Comba, 3000-548 Coimbra, Portugal
Phone: +351 239 488510
E-mail: mcbranco@fmed.uc.pt

Otília C. d'Almeida: **E-mail:** oalmeida@fmed.uc.pt

Abstract

Adult neural plasticity within the visual system remains controversial. Starkly opposing views still remain on the ability of the visual system to reorganize in adulthood. Most attempts have focused on testing reorganization upon central visual loss. However, central loss triggers immediate adaptive strategies such as the emergence of new retinal preferential fixation loci, which may preclude plasticity. Moreover, plasticity may be further reduced in later ageing periods. Here we addressed this issue by studying visual plasticity in a genetically determined retinal disorder, Retinitis Pigmentosa, in which *peripheral* visual loss emerges not long after the critical period, in teenage years. **We performed a case-control study with one-to-one matching and used an artificial scotoma approach which carefully simulated the defective visual field of each RP patient on a normal-sighted control. We used as outcomes population receptive field measures to probe long-term plasticity using fMRI retinotopy**. We found evidence for reorganization based on **pRF size metrics and explained variance of reorganized visual field maps.** In sum, visual cortical plasticity triggered by peripheral visual loss occurs beyond the critical period of visual maturation.

Keywords

Population receptive fields; plasticity; visual loss; retinitis pigmentosa; scotoma; MRI

Abbreviations

V1: primary visual area; RP: Retinitis Pigmentosa; pRF: population receptive field; FULL: full-field control, SCOT: artificial scotoma control

1. Introduction

The brain is continuously challenged by changes in visual experience. These may lead to short-term or even long-term reorganization and distinct forms of neuroplasticity [1]. Neuroplasticity is an umbrella term describing long-term functional and/or structural changes within the brain. Accordingly, the nervous system is able to adapt itself by modulating its neural activity and subsequently reorganizing its functions and/or micro- and macrostructure triggered by external or internal stimuli. However, beyond the critical windows of development, during which the brain has an innate ability to reorganize itself functionally and/or anatomically, neural plasticity is a particularly controversial phenomenon [2].

This is the case for low level visual cortical regions (for a review see Castaldi et al., 2020), both in animals and humans, especially after the critical period. Several approaches have been proposed to provide quantitative markers of cortical plasticity in humans, such as ocular dominance changes following brief periods of monocular deprivation, assessed by binocular rivalry paradigms [4] and pupillometry [5], visual evoked potentials [6], and measures derived from BOLD-fMRI [7,8].

The visually impaired brain provides a unique opportunity to investigate the mechanisms of neural plasticity in the adult. Since early visual cortex has a retinotopic and hierarchical architecture, that is set from early childhood [9,10], neural visual population receptive field (pRF) properties may represent objective indicators of cortical organization [11], as pRF mapping is a valuable asset to evaluate visual map topology independently from subjective perception [12]. Recent techniques allow to estimate more fine-scaled properties of pRFs, namely their position and size along visual areas [13–15].

Prior animal studies found enlarged pRF sizes and shifts in retinal topography after inducing retinal and cortical lesions in adult cats and monkeys suggestive of neuroplasticity [16]. On the other hand, some authors found no evidence for primary visual area (V1) reorganization after binocular retinal lesions on macaques within 7.5 months, evaluated by fMRI and corroborated by electrophysiology measurements [17]. These inconsistencies [2] render the controversy in human studies even more intriguing.

Retinitis Pigmentosa (RP) is a genetically-determined retinal disease characterized by photoreceptor loss in which age of clinical onset is usually well after the critical period (in teenage years and beyond) and prior to age-related changes [18,19]. With the course of the disease, regions of visual loss (scotomas) appear in the periphery. If

therapeutic solutions emerge, it is of utmost importance to understand how they will interact with potential cortical plasticity. Here we directly asked if signatures of adult plasticity are present in RP by investigating **the dichotomy of stability *vs*. plasticity** of pRF sizes in early visual areas. Often these two concepts have been used interchangeably, yet some subtle differences should be considered, mostly related to the temporal scale of the cause/effect events and their reversibility [2]. To disentangle between long-term plasticity and short-term adaptation, we designed a one-to-one matched case-control approach by artificially simulating the defective visual field of each RP patient on a normal-vision control while measuring pRFs. Such artificial scotoma approach is considered to be the ideal approach to separate short-term effects from true plasticity [20,**21**]. If plasticity is absent, similar pRF size patterns should be found in RP and matched controls.

2. Materials and methods

2.1. Participants

A total of 37 participants belonging to three independent groups enrolled in this experiment (Table 1): the Retinitis Pigmentosa (RP) group, included 12 patients recruited in collaboration with the Ophthalmology Unit, Coimbra Hospital and University Centre, Portugal; the full-field control group (FULL), included 13 normally sighted participants that performed the original protocol (as the RP group); and the artificial scotoma control group (SCOT), an independent control group including 12 normally sighted participants submitted to an artificially-simulated scotoma fMRI experiment (more details below). All 25 control participants were recruited from a volunteers' database. **The sample size was based on previous studies [12,22–24] and is actually one of the largest in the literature.** The study was approved by the Ethics Commission of the Faculty of Medicine, University of Coimbra, and was conducted in accordance with the Declaration of Helsinki. Written informed consent was obtained from all participants after all procedures were explained.

A general ophthalmological screening was performed including visual acuity assessment, frequency-domain Cirrus Optical Coherence Tomography (OCT, software version 5.1.1.6, Carl Zeiss Meditec AG, USA) to estimate retinal fiber layer and average retinal thickness, and standardized static visual field perimetry (MonCv3 multifunction perimeter, Metrovision, France)**, as described in [22].** The latter allowed not only to evaluate the

extent of visual field damage (mean deficit and visual field diameter), estimated from the sensitivity values (dB) of each visual area position tested, but also to obtain visual field sensitivity maps to be used in the artificial scotoma experiment.

Exclusion criteria included visual field diameter smaller than 5º and/or visual acuity lower than 0.2 in both eyes that would result in fixation difficulties during visual examinations and fMRI acquisitions.

	RP	FULL	SCOT	***Statistics***
N	12	13	12	
Age (y)	33.9±8.31	33.2±9.80	34.0±7.02	$F_{(2,34)}$**=0.04, *p*=0.963**
Sex (Male:Female)	9:3	9:4	9:3	χ^2**=0.142, *p*=0.931**
Selected eye (Left:Right)	5:7	5:8	5:7	χ^2**=0.036, *p*=0.982**
Disease duration (y)	21.3±10.25	-	-	-
Visual Acuity[a] (logMAR)	**0.2±0.11**	**0.0±0.07**	**0.0±0.06**	***H*=24.8, *p*<0.001[b]**
Visual Angle[a] (diameter, deg)	17.1±13.84	49.8±4.51	54.0±6.27	***H*=27.6, *p*<0.001[b]**
Mean Deficit[a] (dB)	17.4±6.60	0.1±0.40	0.5±0.91	***H*=23.5, *p*<0.001[b]**
Retinal Thickness[a] (µm)	239.0±23.30	285.5±14.23	285.6±7.70	$F_{(2,34)}$**=32.9, *p*<0.001[b]**
RNFL Thickness[a] (µm)	107.0±15.23	95.3±10.53	95.5±10.90	$F_{(2,34)}$**=3.6, *p*=0.039[c]**

RNFL, Retinal nerve fiber layer
Quantitative data is presented as mean±SD and qualitative data as frequencies
[a] Mean of left and right eye values
[b] **Pairwise *post-hoc* tests (Bonferroni corrected) showed s**tatistical differences between RP and both control groups
[c] **Pairwise *post-hoc* tests (Bonferroni corrected)** showed no pairwise statistical differences between groups

Table 1. Clinical-demographic data of the three cohorts: Retinitis Pigmentosa (RP), the full-field control (FULL), and the artificial scotoma control (SCOT) groups**. Statistical significance value (*p*-value) refers to the comparisons accross the three groups.**

2.2. MRI data acquisition and experimental design

2.2.1. Neuroimaging acquisition

MRI data was acquired using a 3T Siemens Magnetom TrioTim scanner (Siemens AG, Germany) at the Portuguese Brain Imaging Network with a 12-channel birdcage head coil. The acquisition protocol consisted of two high-resolution T1-weighted 3D Magnetization Prepared Rapid Acquisition Gradient Echo (MPRAGE) sequences and four functional MRI runs (two polar angle (PA) and two eccentricity (Ecc) stimuli, acquired in alternated runs, PA-Ecc-PA-Ecc). The acquisition parameters were as following: MPRAGE, 176 slices with 1 mm

isotropic voxel, repetition time/echo time (TR/TE) 2530/3.42 ms, flip angle (FA) 7°, field of view (FoV) 256×256 mm^2; fMRI runs, 26 slices using a single shot Echo-Planar Imaging sequence acquired in the axial plane parallel to the anterior commissure-posterior commissure (AC-PC) plane with a 2 mm isotropic voxel, TR/TE 2000/39 ms, interslice time (TI) 76 ms, FA 90°, FOV 256×256 mm^2, 128×128 imaging matrix**, 108 volumes per run**. All anatomical data was inspected by a neuroradiologist to exclude potential structural alterations. MRI-compatible goggles with refractive correction (VisualSystem, NordicNeurolab, Norway) were used to present the retinotopy stimuli. The experimental procedure was performed monocularly using the dominant eye, determined using the Dolman hole-in-the-card test, except if it had the lowest visual acuity, to reduce discomfort during the acquisition. The non-stimulated eye was covered with a cotton patch. Fixation was monitored synchronously during the acquisition by the operator with an eye-tracker device (EyeTracking Camera, NordicNeurolab, Norway).

2.2.2. Experimental design

The stimuli and experimental design for fMRI paradigms were developed using MATLAB (R2011b, The MathWorks, USA) and Psychophysics Toolbox 3 extensions for MATLAB (http://psychtoolbox.org/).

In MRI, the maximum field of view was 23°×30°. The stimuli (Fig. 1A) used for population receptive field (pRF) estimation consisted in conventional single 45° counter-clockwise rotating wedge (polar angle) and expanding ring (eccentricity) with a high-contrast (~100%) flickering (8Hz) checkerboard pattern in agreement to standard retinotopic paradigms first described by Sereno et al. (1995). Both stimuli moved across the visual field in 24 discrete steps, 2s in each position spanning all area within 48s. Each run had a 12s initial fixation block (6 TR) of mean luminance with zero contrast (~20 cd/m^2) and 12s mean luminance blocks of zero contrast inserted within the two middle cycles replacing the stimuli in 6 consecutive TR to estimate population receptive fields with the modelling method described by Dumoulin and Wandell [13]. The order of the insertion of mean luminance blocks is depicted in Fig. 1A (as binary stimulus frames). The participants were asked to keep fixation in a central red cross with 0.78° of diameter.

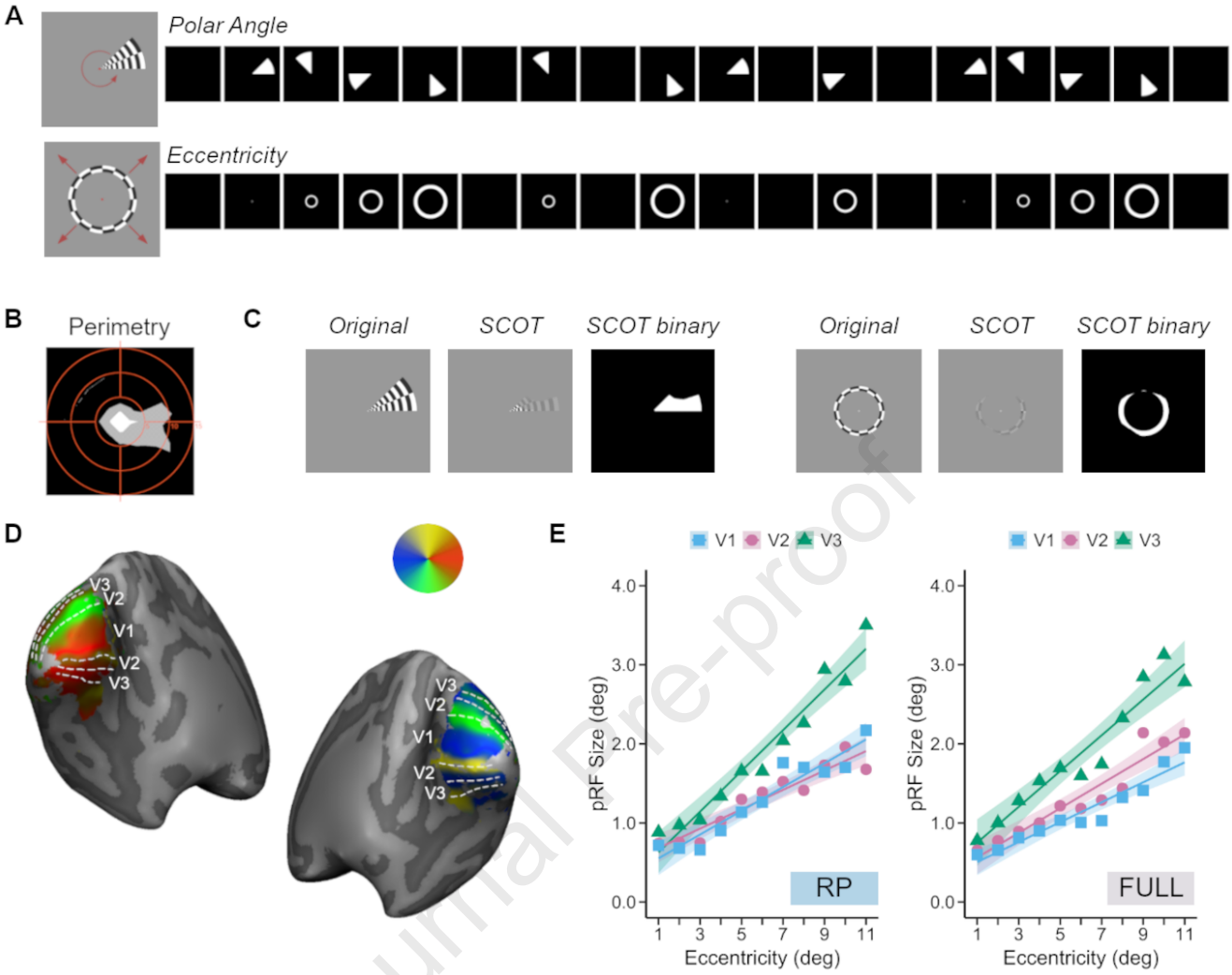

Fig. 1. Population receptive field (pRF) mapping. **(A)** Modified versions of standard retinotopy experiments of the polar angle (rotating wedge) and eccentricity (expanding ring) stimuli were used, including the insertion of mean luminance periods replacing different positions of the retinotopy stimulus. Protocols of each run are presented as binary frames (each 12s frame, 6×TR). **(B)** Visual field perimetry data of retinitis pigmentosa (RP) patients were collected to create artificial scotoma masks. In the representative perimetry map, black-to-white represents lower-to-higher sensitivity areas, and concentric rings mark 5°, 10° and 15° (radius) from the center. A low-pass filter was used to get smooth transitions along the sensitivity maps. **(C)** Controls from the artificial scotoma group (SCOT) were submitted to a modified version of the original stimuli by applying a mask based on the perimetry data of the matched RP patient (as a strategy to simulate the visual field perception of the patient). When creating the binary masks for pRF estimation, all visible areas were considered as a stimulated region (white). **(D)** Early visual areas, V1, V2, and V3, were manually defined according to individual functional polar

angle maps overlaid on inflated meshes of the left and right hemispheres (representative data). **(E)** Linear regression lines were adjusted for the average pRF size (deg) in each 1° equally spaced eccentricity bin (Bin 1, 0.5°-1.5°; Bin 11, 10.5°-11.5°) in each visual area: V1 (blue circles), V2 (pink squares) and V3 (green triangles) for the full-field controls with normal vision (FULL) and Retinitis Pigmentosa (RP) groups. Shaded areas represent 95% confidence bands of best-fit regression lines for each visual area.

2.2.3. Artificial Scotoma stimuli

To resolve chronic from acute adaptive effects we performed a matched case-control artificial scotoma experiment (Fig. 1C), by adapting the original retinotopy stimulus and presenting it to an independent control group (SCOT). Each SCOT participant was age- and sex-matched to a RP patient (Table 2). In the MRI, the SCOT participant was presented to a polar angle and an eccentricity stimulus masked by the perimetry visual field sensitivity map of the corresponding RP patient (Fig. 1B). A circular averaging filter was applied to create a soft blur based on the field deficit preventing sharp borders (Fig. 1C).

ID	Subgroup	Age (y)	Sex	Handedness	Stimulated Eye	Visual angle[a] (deg)	Onset age (y)	Disease Duration (y)
RP1	RP	19	M	R	L	14.5	7	12
RP2	RP	23	M	R	R	8.5	16	7
RP3	RP	24	M	R	R	43.0	14	10
RP4	RP	31	M	R	L	47.5	2	29
RP5	RP	34	F	R	R	15.5	3	31
RP6	RP	35	M	R	L	9.5	6	29
RP7	USH	34	F	R	R	9.0	14	20
RP8	RP	37	F	R	L	21.5	32	5
RP9	RP	41	M	R	L	8.0	18	23
RP10	USH	42	M	R	R	9.0	14	28
RP11	USH	44	M	R	R	7.5	18	26
RP12	USH	43	M	R	R	13.0	8	35
SCOT 1		24	M	R	L	60.0		
SCOT 2		25	M	R	R	60.0		
SCOT 3		27	M	R	R	48.0		
SCOT 4		28	M	R	L	60.0		
SCOT 5		31	F	R	R	48.0		
SCOT 6		34	F	R	R	48.0		
SCOT 7		34	M	R	L	60.0		
SCOT 8		39	F	L	L	60.0		
SCOT 9		39	M	R	L	48.0		
SCOT 10		40	M	R	R	48.0		
SCOT 11		43	M	L	R	60.0		
SCOT 12		44	M	R	R	48.0		

F, female; *L*, left; *M*, male; *R*, right; *USH*, Usher Syndrome

[a] Visual angle diameter (deg) of the eye opened during fMRI

Table 2. Summary of the individual clinical-demographic characterization for all the participants from the Retinitis Pigmentosa (RP) and the artificial scotoma (SCOT) control groups.

2.3. fMRI data processing and analysis

2.3.1. MRI data pre-processing

All MRI data were preprocessed and analyzed using BrainVoyager . Each anatomical dataset was skull-stripped and corrected for intensity inhomogeneities, and then averaged to improve the signal-to-noise ratio. The resulting volumes were re-oriented to the AC-PC plane and normalized to Talairach coordinate space. An automatic segmentation routine was applied to separate gray and white matter and then to create 3D triangular mesh

representations of each hemisphere. To project the functional maps in a fully exposed cortical surface, each reconstructed and morphed hemisphere was inflated.

Each fMRI dataset was pre-processed with mean intensity correction, slice scan time correction (trilinear/sinc interpolation), rigid-body 3D interscan motion correction, and temporal high-pass filtering (2 cycles per run). Runs with motion parameters' estimates higher than 3 mm translation or 3° rotation in any direction were discarded from analysis. Only the first eccentricity run of an RP participant was excluded. Due to the use of preparation scans, none of the initial volumes needed to be discarded to account for early magnetization transients. All preprocessed functional runs were coregistered to the Talairach anatomical images and pRF estimation was performed in surface space directly.

2.3.2. Retinotopic mapping and pRF estimation

To estimate the size of the pRF and obtain eccentricity and polar angle maps we used the Dumoulin and Wandell model-driven approach [13] implemented in BrainVoyager. Accordingly, the pRFs response was described by a 2D gaussian [26] with three free parameters, the positions x and y, and the spread/standard deviation (pRF size). Stimuli frames were binarized by eliminating the checkerboard pattern (Fig. 1C) and downsampled to 300×300 px. In the SCOT group, only areas of absolute scotoma (sensitivity below 10 dB) were set in black, and all visible area was considered as a stimulated region (white). To calculate the optimal pRF parameters, a grid-search approach was used to estimate 27000 candidate configurations (30×30, x and y positions, extending from -11.5° to 11.5° within a 23°×23° visual field). The pRF sizes were assumed to vary with increasing spreads from 0.2° to 7.1° in 30 equal steps. The estimation was restricted to the posterior region encompassing the occipital lobe. The explained variance (R^2) was used as a quantitative measure of the goodness-of-fit of the fMRI pRF modeling**. To reduce the influence of noisy vertices, pRF sizes were extracted only from voxels with R^2≥10%.**

It is known that retinotopic areas V1, V2 and V3 can be defined relative to the vertical and horizontal meridians in a mirror/non-mirror configuration. We therefore overlaid the polar angle map over the individual 3D meshes of each hemisphere and manually defined these regions-of-interest (ROIs) using BrainVoyager's surface drawing tools (Fig. 1D).

Mean pRF size was estimated as the average of all vertices inside each functionally defined low-level visual areas V1, V2, and V3, for each eccentricity bin. Eccentricity bins were defined each 1° ranging from 0.5° (bin 1, 0.5°-1.5°) to 11.5° (bin 11, 10.5°-11.5°). Some participants had missing data in some bins due to the application of outlier quality criteria. Additionally, calcarine sulcus was manually drawn from anatomical curvature maps for all cases as a proxy of primary visual area, V1 (Fig. 2B), since the low pRF fMRI signal of several artificial scotoma control (SCOT) participants prevented the functional definition of V1, V2 and V3 (Fig. 2A).

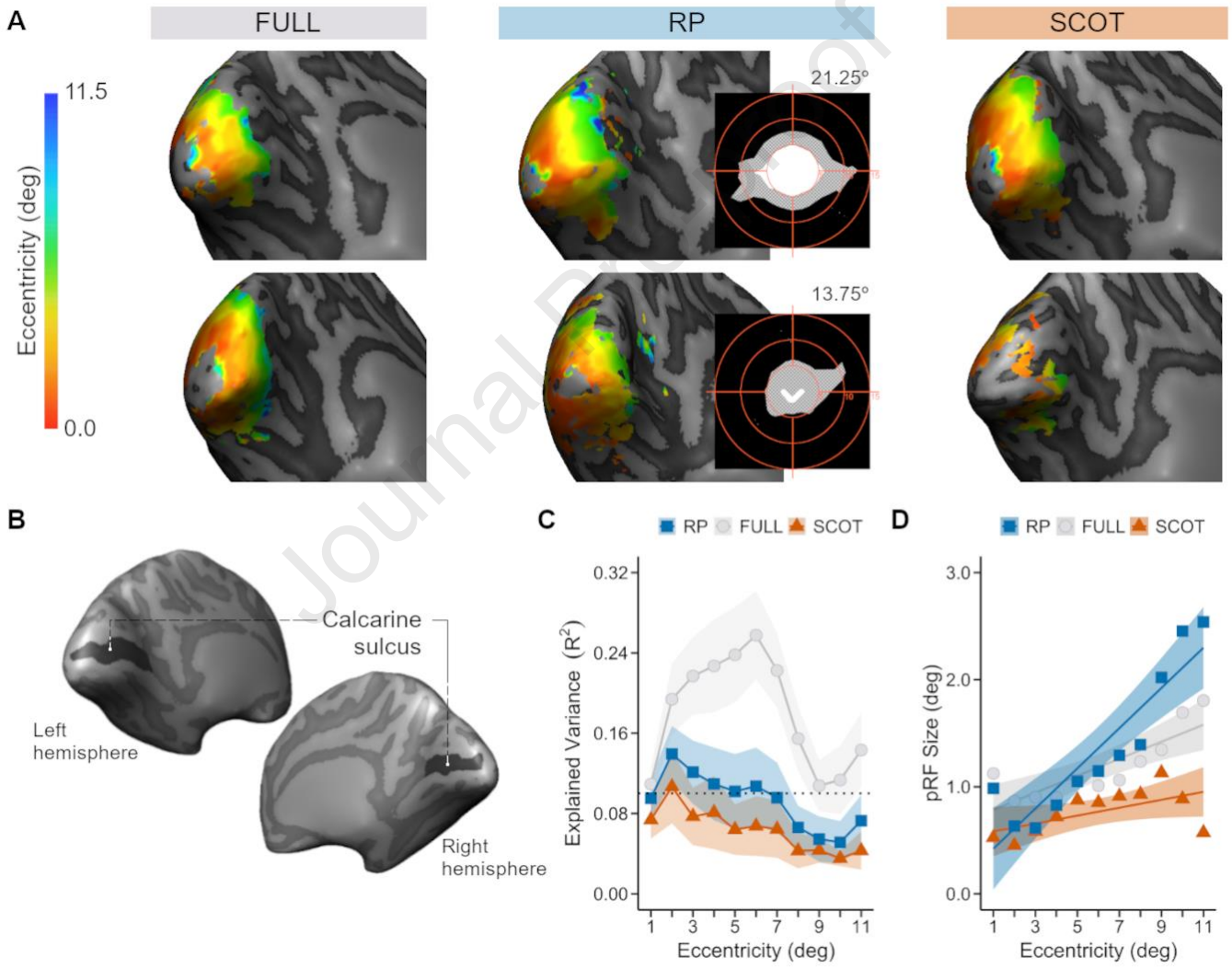

Fig. 2. Illustrative eccentricity functional maps of six participants and evaluation of the model fitting along the calcarine sulcus as an approximation of V1. (A) Eccentricity (deg) maps of the left hemisphere of matched participants (rows) of the three groups: full-field control (FULL), Retinitis Pigmentosa (RP), and artificial scotoma

control (SCOT), overlaid over inflated meshes. Perimetric visual field maps of the left eye, with the respective mean visual angle diameter, of each RP patient are depicted in the insets, where each circle is positioned at 5°, 10°, and 15° (radius) from the center (white to black regions correspond to high to low visual field sensitivity). At the bottom row, notice the residual signal in the SCOT participant, while the RP patient still exhibits a reduced but preserved signal in the presence of a small visual field. Smoothing in the cortical functional maps was used for visualization purposes only. **(B)** Calcarine sulcus (dark-grey) was anatomically defined based on the curvature maps over inflated left and right hemisphere meshes of each individual. **(C)** Mean explained variance (R^2) was used as a goodness-of-fit measure of the pRF model along equally spaced eccentricity bins (bin 1, 0.5°-1.5°; bin 11, 10.5°-11.5°) in the anatomically defined calcarine sulcus of RP (blue squares), SCOT (orange triangles) and FULL (light grey circles) groups. Markers and shaded areas represent, mean R^2 and 95% confidence interval for each group. The dotted line at 10% marks the threshold set in the previous functional definition of the regions-of-interest in RP and FULL groups. **(D)** To evaluate the pRF size modulation along eccentricity in RP and SCOT groups, linear regression lines were adjusted and compared between groups**. In panel A, a threshold of R=0.030 was applied to the functional maps.** Markers and shaded areas represent pRF size (deg) within each eccentricity bin and 95% confidence bands of best-fit regression lines for each group. See also Appendix, Fig. A.1.

2.4. Statistical analysis

Population receptive field maps features were retrieved with the MATLAB-based (MATLAB R2020a, v9.8.0, The MathWorks, USA) BVQXtools/NeuroElf (by Jochen Weber; http://neuroelf.net/) toolbox and in-house MATLAB scripts. ROIs were divided into eccentricity areas (bins) ranging from 0.5° to 11.5° in 1° steps (eccentricity bins). PRF sizes from each ROI of each hemisphere were extracted for each eccentricity bin. **Only vertices for which explained variance $R^2 \geq 10\%$ were further considered.** In analysis of explained variance, all not null values were considered.

Statistical analysis was performed using IBM SPSS Statistics for Windows, version 28 (IBM Corp., Armonk, N.Y., USA), otherwise stated. Qualitative variables were analyzed with χ^2 independence test. Linear regression fitting was applied for mean pRF size along eccentricity in each ROI of each group. Comparison of the slope and

y-intercept of regression lines for V1, V2 and V3 of RP and FULL groups was independently performed using Prism version 6.0.0 for Windows (GraphPad Software, La Jolla California, USA), using ANCOVA. GLM repeated measures ANOVA (rmANOVA) was used to compare the differences of mean R^2 values along eccentricity in anatomically defined calcarine sulcus (manually drawn from curvature maps) between RP, and both control groups (FULL and SCOT). When assumptions of sphericity were not met, the Huynh–Feldt ($\varepsilon > 0.75$) or the Greenhouse–Geisser ($\varepsilon \leq 0.75$) corrections were selected. Bonferroni correction was used for post-hoc multiple comparisons testing. Partial eta-squared (η_p^2) was used to evaluate the effect size of the *F*-tests. Regression lines were fit to mean pRF sizes along eccentricity bins in the calcarine sulcus of each cohort and an ANCOVA was applied to compare slopes between RP and SCOT groups. **Exploratory correlation analysis between disease course and retinal indicators (age of disease onset, disease duration, and retinal and RNFL thickness) and summary measures of pRF size (mean pRF size, slope and y-intercept of the mean pRF size *vs.* eccentricity regression lines in V1, V2, V3 and calcarine sulcus) were also performed using Spearman's and Pearson correlation testing as appropriate.**

All statistics are presented as the mean ± *SEM* (standard error of the mean) or mean and 95% Confidence Interval, as appropriate. Two-tailed hypothesis testing was performed at 5% significance level.

3. Results

In our study, three independent groups were considered: RP, the case group, including patients diagnosed with Retinitis Pigmentosa; FULL, a normal-vision control group, including subjects without RP submitted to the same fMRI stimulation protocol (full field) as RP; SCOT, an independent normally sighted control group that was presented with an adapted retinotopy paradigm, masking the scotoma region and simulating the functional visual field loss of an age- and gender-matched RP patient.

3.1. Descriptive characterization of retinotopic organization

In this section and before testing our main hypothesis in the next section we provide a description of retinotopic organization. Modified versions of the polar angle and eccentricity retinotopy paradigms (Fig. 1A) were used to functionally define early visual areas V1, V2 and V3 (Fig. 1D) and to estimate pRF sizes along eccentricity. Linear regression lines were adjusted to the mean pRF size values along eccentricity for each visual area in RP (Fig. 1E). An analysis of covariance (ANCOVA) on mean pRF size between visual areas V1-V3, having eccentricity as a covariate was performed to compare regression slopes. We found the expected significant interaction visual area×eccentricity ($F_{(2,642)} = 11.91$, $p = 8.00\times10^{-6}$, $\eta_p^2 = 0.04$) indicating a difference between regression line slopes. *Post hoc* tests showed statistically significant differences between V1 and V3 ($F_{(1,433)} = 12.10$, $p = 5.56\times10^{-4}$, $\eta_p^2 = 0.03$) and V2 and V3 ($F_{(1,413)} = 26.91$, $p = 3.35\times10^{-7}$, $\eta_p^2 = 0.06$). Interestingly, there were no differences between either the slopes or regression line y-intercepts between V1 and V2.

Analysis with people with normal vision, hereafter named FULL group, the evolution of the pRF sizes across visual areas V1, V2 and V3 and within these areas (along eccentricity) followed the expected pattern, with a significant difference between regression line slopes (area×eccentricity: $F_{(2,834)} = 10.79$, $p = 2.40\times10^{-5}$, $\eta_p^2 = 0.03$). *Post-hoc* analysis showed that between V1 and V2, slopes were not statistically different but the difference between the y-axis intercepts of V1 and V2 regression lines was statistically significant ($F_{(1,560)} = 9.20$, $p = 0.003$, $\eta_p^2 = 0.02$). Also, there was a statistically significant difference (*post-hoc*) between V3 and both V1 ($F_{(1,557)} = 20.63$, $p = 7.00\times10^{-6}$, $\eta_p^2 = 0.04$) and V2 ($F_{(1,552)} = 9.58$, $p = 0.002$, $\eta_p^2 = 0.02$).

3.2. The nature of PRF organization along the calcarine sulcus in RP patients but not in artificial scotoma suggests long-term plasticity

In this section we test the main hypothesis of our study. To simulate the perceived visual field of each RP patient, a matched control (SCOT) undergone fMRI scanning with a modified version of the original stimuli. Briefly, the polar angle and eccentricity stimuli was masked according to the visual field sensitivity map of the matching RP patient estimated by perimetry (Fig. 1B,C). The expected weak signal (Fig. 2A) in most of the SCOT participants (normally sighted controls with a simulated artificial scotoma), prevented a clear-cut functional definition of early visual areas. To circumvent this challenge posed by artificial scotomas, and to avoid bias, the calcarine sulcus was

anatomically delimited based on the curvature maps along primary visual area V1 (Fig. 2B). Explained variance (R^2) maps were used as a primary quantitative metric to evaluate the goodness-of-fit of the pRF signal [13]. According to our hypothesis, a higher value than predicted by artificial scotomas after visual loss suggests more robustly preserved or improved retinotopic representations. If these values are larger in RP than in SCOT, this would indicate reorganization in the former. Mean R^2 (values > 0) in each 1° eccentricity bin along calcarine sulcus (Fig. 2C) were estimated for all participants (RP, FULL, SCOT).

A two-way rmANOVA was applied on R^2 mean values with eccentricity as a within-subjects factor and the group as between-subjects factor (Fig. 2C). A significant interaction eccentricity×group was found (${}_{GG}F_{(12.2,415.2)} = 4.75$, $p = 2.18\times10^{-7}$, $\eta_p^2 = 0.12$). As expected, R^2 was, in general, significantly lower for RP when compared to the FULL group (except for the most central eccentricities, bins 1 and 2, Bonferroni corrected). Generally, R^2 was consistently lower in SCOT, and, supporting our hypothesis, higher in the RP and FULL groups. The main effect of group ($F_{(2.0,68.0)} = 26.70$, $p = 2.76\times10^{-9}$, $\eta_p^2 = 0.44$) was further supported by post-hoc analyses, with even stronger effects when removing the two SCOT participants matching RP patients with visual field diameter higher than 23°. This sensitivity analysis (Appendix, Fig. A.1) showed significant eccentricity×group and group effects (interaction: ${}_{GG}F_{(12.0,383.3)} = 5.74$, $p = 3.96\times10^{-9}$, $\eta_p^2 = 0.15$; group: $F_{(2.0,64.0)} = 38.15$, $p = 1.24\times10^{-11}$, $\eta_p^2 = 0.54$). Bonferroni-corrected post-hoc analysis disclosed significantly lower pRF sizes in SCOT group compared to RP for more central bins 2 and 3 (1.5° to 3.5°) and bin 7 (6.5° to 7.5°).

To further confirm this effect, since this study followed a one-to-one matched case-control (RP to SCOT) approach, a bin-wise sign test was applied, given that bins are paired for mean R^2 values of each patient and matched SCOT individuals (for each eccentricity of each hemisphere). The sign tests showed statistically significant differences between the two medians in most central eccentricities (0.5°-1.5°, 2.5°-7.5°, *p*-values ranging from <0.001 to 0.007) in which mean R^2 was, in general, lower for SCOT individuals, suggesting that "reorganization" cannot be explained by an artificial scotoma. Since two RP patients had perimetric visual angles larger than 23°, the matched SCOT individuals were presented with regular pRF mapping stimulus as resembling FULL participants, because of the preserved vision in those cases. This would possibly influence both R^2 and pRF size estimates and reduce real group differences, being more conservative. Sensitivity analyses (Appendix, Fig.

A.1) were further considered considering the level of visual preservation without the mentioned pairs. Sign tests showed significantly lower R^2 for SCOT individuals in all central areas (0.5°-7.5°, p-values ranging from <0.001 to 0.041) and 10.5°-11.5° ($p = 0.041$).

To find an independent metric of reorganization, pRF sizes were averaged for each eccentricity bin along the calcarine sulcus for vertices with $R^2 > 0$. Analysis of the regression lines adjusted to the mean pRF size along eccentricity in the calcarine sulcus of RP and SCOT groups (Fig. 2D) showed a significant difference between slopes ($F_{(1.0,296.0)} = 15.01$, $p = 1.32\times10^{-4}$, $\eta_p^2 = 0.05$), suggesting that group differences amplify at larger eccentricities, as expected from the locus of reorganization. Slopes of the mean pRF size vs. eccentricity regression lines remained different between RP and SCOT groups ($F_{(1.0,254.0)} = 8.42$, $p = 0.004$, $\eta_p^2 = 0.03$), even when removing the two SCOT controls matching RP who had visual preservation beyond 23°.

3.3. PRF size is not associated with disease course and retinal measures

Exploratory correlation analyses between each summary measures representing the pRF size (average pRF size, slope and y-intercept) in each ROI (calcarine sulcus, V1,V2 and V3) and disease duration and onset, and RNFL and retinal thickness of RP patients showed no statistically significant effects.

4. Discussion

We found evidence for long-term residual functional neuroplasticity in adult visual cortex of Retinitis Pigmentosa patients, a genetic model of visual field loss after the critical period. This reconciles evidence from animal models that had remained difficult to demonstrate in humans.

In animal model studies direct manipulations of sensory input are implemented by inflicting circumscribed lesions at the retinal or cortical level. Pioneering research in adult cats and macaque monkeys evidenced that after retinal deafferentation, short-term functional adaptations occur adjacent to the cortical lesion projection zone in which ectopic receptive fields become significantly enlarged, even though having a weaker signal [27,28].

In humans, neuroplasticity research hinges on models of pathologic sensory deprivation or loss [8,29]. **Yet, the** identification of short-term changes does not necessarily imply plasticity. **In a study with RP patients, authors found evidence for a short-term adaptive processes using a monocular deprivation approach in a binocular rivalry task, in which patients with greater impairment presented stronger effects [30]. Another study using fMRI** phase-encoded retinotopic mapping showed that in primary visual cortex (V1) of RP patients, central retinal inputs were shifted towards the periphery (with lower retinal input), in the absence of cortical thickness changes, also suggestive of functional reorganization mechanisms [22]. Similar to the former [30] the degree of remapping was associated with the magnitude of the visual loss in which larger remapping could be related to smaller visual fields. However, no evidence for long-term changes and true plasticity could be shown.

In a seminal inaugural study with two macular degeneration patients, with extensive macular damage leading to loss of central vision, evidence for large-scale reorganization was found as peripheral visual field stimulation elicited BOLD activation at the occipital pole but not in normal-vision controls [31]. Remarkably, in a follow up study, the authors found that this neural reorganization is also dependent on the extension of the retinal lesion, evident only in the patient with total absence of foveal input [32]. On the other hand, in a study conducted by Baseler et al. (2011), no evidence for cortical remapping was found in a larger cohort of macular degeneration patients.

The controversy underlying previous studies may relate to the difficulty in showing plasticity in central visual loss [11] because adaptive behavioral strategies (e.g. training new preferred fixation loci) may hinder neuronal reorganization processes, which should not be the case for peripheral lesions. The inconsistency of results on cortical neuroplasticity may also stem from other factors including clinical individual variability [33], as well as methodological heterogeneity such as study design, and the lack of clear indicators of plasticity.

In our work, we found clear-cut evidence for long-term reorganization, while the general increase of pRF along eccentricity was observed both in Retinitis Pigmentosa and control individuals, as expected, being smaller in V1 and higher in V3 [11]. Nonetheless, the question on the timescale of these mechanisms and if they indicate genuine plasticity remains unanswered, i.e., a putative remapping in the visual cortex of RP patients is a marker of ‘short term adaptation’ or ‘plasticity’?

We therefore manipulated the visual input to simulate the visual field of the patients by masking the stimulus according to VF perimetry, the so-called *artificial scotoma* approach**, framing a more adequate control to study pRF characteristics of patients [21]. This method intends to simulate a retinal lesion in normally sighted participants removing parts of the stimulus within the visual field [11,14,20,34]. In our sensitive one-to-one matching approach, each RP patient was age- and sex-matched to a normal sighted control participant that was presented with an adapted pRF stimuli based on the perceptual experience of the matched patient (using the perimetric visual field to simulate the retinal lesion).** By hypothesis, if fast adaptation occurs, the neuronal maps would swiftly reflect the recent lack of sensory input. However, if long-term neuroplasticity takes place, by hypothesis, a distinctly organized retinotopic signal would be, at least partially, present in the patients, in contrast with the artificial scotoma controls.

We found that, in general, RP patients showed evidence for a more organized visual map as compared to artificial scotoma which was contingent on the amount of visual field loss. Moreover, the pRF dependence on eccentricity also changed, suggesting larger peripheral pRFs in patients, as predicted by animal studies. Artificial scotoma pRF mapping excludes rapid adaptation and suggests instead long-term plasticity mechanisms.

Previous small sized studies in disorders not specifically affecting the photoreceptor layer such as choroidemia analyzed pRFs from a clinical point of view but not plasticity [35]. We [23] and others [24] had also investigated other factors such as attention mechanisms. One should also consider prior studies in central vision [31,32], but here we studied peripheral vision loss, where compensatory mechanisms that occur near the fovea, such as preferential fixation do not exist.

Some considerations must be considered when interpreting the results. First, to create the masks for the SCOT group, we used standardized static visual field perimetry to define the boundaries of the scotoma of each RP patient. The mask was superimposed over the retinotopic stimuli aiming to mimic the perceived visual field of RP patients. A smoothing filter was applied to prevent sharp borders. However, it is impossible to guarantee perfect masking. Still, we believe that this approach is more ecological than a coarse definition of the scotoma area (e.g., circular [34] or quadrant [15]). **Second,** the parameters of the assumed hemodynamic response function may affect pRF modeling but only absolute, and not relative, pRF size estimates [13] in within group designs**. Last, men are affected slightly more than women, limiting analysis of potential sex-related effects.**

5. Conclusion

Functional remapping upon visual loss remains controversial in adulthood, as well as if it reflects true plasticity. We tested this hypothesis in Retinitis Pigmentosa where peripheral retinal loss does not lead to novel fixation loci facilitating the demonstration of plasticity. By using a matched one-to-one scotoma mapping approach in this genetically determined retinal disorder we found strong evidence for long-term reorganization based on population receptive field modelling statistics. Our results align with the view of visual cortical plasticity triggered by peripheral visual loss after the critical period of visual maturation.

Funding

This work was supported by the Portuguese Foundation for Science and Technology (FCT) with the following grants: E-Rare2-SAU/0001/2008, e-Rare4/0001/2012, COMPETE, POCI-01-0145-FEDER-00744, FCT/UIDB&P/4950/2020, FCT/2022.02963.PTDC, DSAIPA/DS/0041/2020, MEDPERSYST, POCI-01-0145-FEDER-016428, and BIGDATIMAGE, CENTRO-01-0145-FEDER-000016 financed by Centro 2020 FEDER, COMPETE. The sponsor was not involved in neither the study design, data collection, analysis, and interpretation, article preparation and submission for publication.

CRediT authorship contribution statement

Otília C. d'Almeida: Formal analysis, Supervision, Visualization, Writing - original draft, Writing - review & editing. **Joana M. Sampaio**: Formal analysis. **Sonia Ferreira**: Conceptualization, Investigation. **Eduardo D. Silva**: Investigation. **Miguel Castelo-Branco**: Conceptualization, Funding acquisition, Supervision, Writing - review & editing.

Declaration of competing interest

The authors declare that they have no known competing financial interests or personal relationships that could have appeared to influence the work reported in this paper.

Data availability

Data supporting the findings of this study are available from the corresponding author upon reasonable request.

Acknowledgments

We gratefully acknowledge the collaboration of all participants of this study. We also thank Andreia Pereira for assistance in data collection.

Appendix A. Supplementary data

References

[1] A. Pascual-Leone, A. Amedi, F. Fregni, L.B. Merabet, The plastic human brain cortex, Annu Rev Neurosci 28 (2005) 377–401. https://doi.org/10.1146/annurev.neuro.27.070203.144216.

[2] B.A. Wandell, S.M. Smirnakis, Plasticity and stability of visual field maps in adult primary visual cortex, Nat Rev Neurosci 10 (2009) 873–884. https://doi.org/10.1038/nrn2741.

[3] E. Castaldi, C. Lunghi, M.C. Morrone, Neuroplasticity in adult human visual cortex, Neurosci Biobehav Rev 112 (2020) 542–552. https://doi.org/10.1016/j.neubiorev.2020.02.028.

[4] C. Lunghi, D.C. Burr, C. Morrone, Brief periods of monocular deprivation disrupt ocular balance in human adult visual cortex, Current Biology 21 (2011) R538–R539. https://doi.org/10.1016/j.cub.2011.06.004.

[5] P. Binda, C. Lunghi, Short-Term Monocular Deprivation Enhances Physiological Pupillary Oscillations, Neural Plast 2017 (2017) 6724631. https://doi.org/10.1155/2017/6724631.

[6] C. Lunghi, M. Berchicci, M.C. Morrone, F. Di Russo, Short-term monocular deprivation alters early components of visual evoked potentials, Journal of Physiology 593 (2015) 4361–4372. https://doi.org/10.1113/JP270950.

[7] P. Binda, J.W. Kurzawski, C. Lunghi, L. Biagi, M. Tosetti, M.C. Morrone, Response to short-term deprivation of the human adult visual cortex measured with 7T BOLD, Elife 7 (2018) e40014. https://doi.org/10.7554/eLife.40014.

[8] J. Lemos, D. Pereira, M. Castelo-Branco, Visual Cortex Plasticity Following Peripheral Damage To The Visual System: fMRI Evidence, Curr Neurol Neurosci Rep 16 (2016) 89. https://doi.org/10.1007/s11910-016-0691-0.

[9] J. Gomez, V. Natu, B. Jeska, M. Barnett, K. Grill-Spector, Development differentially sculpts receptive fields across early and high-level human visual cortex, Nat Commun 9 (2018) 788. https://doi.org/10.1038/s41467-018-03166-3.

[10] M.B. Hoffmann, S.O. Dumoulin, Congenital visual pathway abnormalities: a window onto cortical stability and plasticity, Trends Neurosci 38 (2015) 55–65. https://doi.org/10.1016/j.tins.2014.09.005.

[11] S.O. Dumoulin, T. Knapen, How Visual Cortical Organization Is Altered by Ophthalmologic and Neurologic Disorders, Annu Rev Vis Sci 4 (2018) 357–379. https://doi.org/10.1146/annurev-vision-091517-033948.

[12] M. Ritter, A. Hummer, A.A. Ledolter, G.E. Holder, C. Windischberger, U.M. Schmidt-Erfurth, Correspondence between retinotopic cortical mapping and conventional functional and morphological assessment of retinal disease, Br J Ophthalmol 103 (2019) 208–215. https://doi.org/10.1136/bjophthalmol-2017-311443.

[13] S.O. Dumoulin, B.A. Wandell, Population receptive field estimates in human visual cortex, Neuroimage 39 (2008) 647–660. https://doi.org/10.1016/j.neuroimage.2007.09.034.

[14] H.A. Baseler, A. Gouws, K. V Haak, C. Racey, M.D. Crossland, A. Tufail, G.S. Rubin, F.W. Cornelissen, A.B. Morland, Large-scale remapping of visual cortex is absent in adult humans with macular degeneration, Nat Neurosci 14 (2011) 649–655. https://doi.org/10.1038/nn.2793.

[15] A. Papanikolaou, G.A. Keliris, T.D. Papageorgiou, Y. Shao, E. Krapp, E. Papageorgiou, K. Stingl, A. Bruckmann, U. Schiefer, N.K. Logothetis, S.M. Smirnakis, Population receptive field analysis of the primary visual cortex complements perimetry in patients with homonymous visual field defects, Proc Natl Acad Sci U S A 111 (2014) E1656–E1665. https://doi.org/10.1073/pnas.1317074111.

[16] U.T. Eysel, G. Schweigart, T. Mittmann, D. Eyding, Y. Qu, F. Vandesande, G. Orban, L. Arckens, Reorganization in the visual cortex after retinal and cortical damage, Restor Neurol Neurosci 15 (1999) 153–164.

[17] S.M. Smirnakis, A.A. Brewer, M.C. Schmid, A.S. Tolias, A. Schüz, M. Augath, W. Inhoffen, B.A. Wandell, N.K. Logothetis, Lack of long-term cortical reorganization after macaque retinal lesions, Nature 435 (2005) 300–307. https://doi.org/10.1038/nature03495.

[18] D.T. Hartong, E.L. Berson, T.P. Dryja, Retinitis pigmentosa, Lancet 368 (2006) 1795–1809. https://doi.org/10.1016/S0140-6736(06)69740-7.

[19] C. Hamel, Retinitis pigmentosa, Orphanet J Rare Dis 1 (2006) 40. https://doi.org/10.1186/1750-1172-1-40.

[20] A. Hummer, M. Ritter, M. Woletz, A.A. Ledolter, M. Tik, S.O. Dumoulin, G.E. Holder, U. Schmidt-Erfurth, C. Windischberger, Artificial scotoma estimation based on population receptive field mapping, Neuroimage 169 (2018) 342–351. https://doi.org/10.1016/j.neuroimage.2017.12.010.

[21] **G.T. Prabhakaran, J. Carvalho, A. Invernizzi, M. Kanowski, R.J. Renken, F.W. Cornelissen, M.B. Hoffmann, Foveal pRF properties in the visual cortex depend on the extent of stimulated visual field, Neuroimage 222 (2020) 117250. https://doi.org/10.1016/j.neuroimage.2020.117250.**

[22] S. Ferreira, A.C. Pereira, B. Quendera, A. Reis, E.D. Silva, M. Castelo-Branco, Primary visual cortical remapping in patients with inherited peripheral retinal degeneration, Neuroimage Clin 13 (2017) 428–438. https://doi.org/10.1016/j.nicl.2016.12.013.

[23] S. Ferreira, A.C. Pereira, B. Quendera, A. Reis, E.D. Silva, M. Castelo-Branco, Enhanced visual attentional modulation in patients with inherited peripheral retinal degeneration in the absence of cortical degeneration, Neural Plast 2019 (2019) 8136354. https://doi.org/10.1155/2019/8136354.

[24] Y. Masuda, H. Horiguchi, S.O. Dumoulin, A. Furuta, S. Miyauchi, S. Nakadomari, B.A. Wandell, Task-dependent V1 responses in human retinitis pigmentosa., Invest Ophthalmol Vis Sci 51 (2010) 5356–64. https://doi.org/10.1167/iovs.09-4775.

[25] M.I. Sereno, A.M. Dale, J.B. Reppas, K.K. Kwong, J.W. Belliveau, T.J. Brady, B.R. Rosen, R.B.H. Tootell, Borders of multiple visual areas in humans revealed by functional magnetic resonance imaging, Science 268 (1995) 889–893. https://doi.org/10.1126/science.7754376.

[26] G. Lerma-Usabiaga, J. Winawer, B.A. Wandell, Population receptive field shapes in early visual cortex are nearly circular, Journal of Neuroscience 41 (2021) 2420–2427. https://doi.org/10.1523/JNEUROSCI.3052-20.2021.

[27] M.A. Gannon, S.M. Long, N.A. Parks, Homeostatic plasticity in human extrastriate cortex following a simulated peripheral scotoma, Exp Brain Res 235 (2017) 3391–3401. https://doi.org/10.1007/s00221-017-5042-0.

[28] B. Dreher, W. Burke, M. Calford, Cortical plasticity revealed by circumscribed retinal lesions or artificial scotomas, in: C. Casanova, M. Ptito (Eds.), Prog Brain Res, 2001: pp. 217–246. https://doi.org/10.1016/s0079-6123(01)34016-5.

[29] B. Röder, R. Kekunnaya, Visual experience dependent plasticity in humans, Curr Opin Neurobiol 67 (2021) 155–162. https://doi.org/10.1016/j.conb.2020.11.011.

[30] C. Lunghi, L. Galli-Resta, P. Binda, G.M. Cicchini, G. Placidi, B. Falsini, M.C. Morrone, Visual Cortical Plasticity in Retinitis Pigmentosa, Invest Ophthalmol Vis Sci 60 (2019) 2753–2763. https://doi.org/10.1167/iovs.18-25750.

[31] C.I. Baker, E. Peli, N. Knouf, N.G. Kanwisher, Reorganization of visual processing in macular degeneration, J Neurosci 25 (2005) 614–618. https://doi.org/10.1523/JNEUROSCI.3476-04.2005.

[32] C. Baker, D. Dilks, E. Peli, N. Kanwisher, Reorganization of visual processing in macular degeneration: Replication and clues about the role of foveal loss, Vision Res 48 (2008) 1910–1919. https://doi.org/10.1016/j.visres.2008.05.020.

[33] E. Ricciardi, D. Bottari, M. Ptito, B. Röder, P. Pietrini, The sensory-deprived brain as a unique tool to understand brain development and function, Neurosci Biobehav Rev 108 (2020) 78–82. https://doi.org/10.1016/j.neubiorev.2019.10.017.

[34] H.D.H. Brown, A.D. Gouws, R.J.W. Vernon, S.J.D. Lawrence, G. Donnelly, L. Gill, R.P. Gale, H.A. Baseler, A.B. Morland, Assessing functional reorganization in visual cortex with simulated retinal lesions, Brain Struct Funct 226 (2021) 2855–2867. https://doi.org/10.1007/s00429-021-02366-w.

[35] E.H. Silson, T.S. Aleman, A. Willett, L.W. Serrano, D.J. Pearson, A.M. Rauschecker, A.M. Maguire, C.I. Baker, J. Bennett, M. Ashtari, Comparing Clinical Perimetry and Population Receptive Field Measures in Patients with Choroideremia, Invest Ophthalmol Vis Sci 59 (2018) 3249–3258. https://doi.org/10.1167/iovs.18-23929.

Long term adult visual plasticity after the developmental critical period in genetically determined *peripheral* visual loss

Highlights

- Functional remapping and adult plasticity after visual loss remain controversial
- We used changes in pRF properties to probe cortical reorganization in Retinitis Pigmentosa
- An artificial scotoma approach was followed to probe long-term neuroplasticity
- Neuroplasticity may occur after peripheral visual loss beyond the critical period

Declaration of interests

☒ The authors declare that they have no known competing financial interests or personal relationships that could have appeared to influence the work reported in this paper.

☐The authors declare the following financial interests/personal relationships which may be considered as potential competing interests: